Systemic RNA oxidation can be used as an index of clinical infection and prognosis in a Vibrio parahaemolyticus Challenge Rat Model

Yaya Pian (pianyaya0919@163.com)
Beijing Hospital https://orcid.org/0000-0002-1519-3947

Jing-Jing Nie
Beijing Hospital

Chen-Chen Wang
Beijing Hospital

Qian Liu
Beijing Hospital

Zhen Liu
Beijing Hospital

Wei Zhang
Beijing Hospital

Li-qun Zhang
Beijing Hospital

Qiu-geng Ou-Yang
Beijing Hospital

Guo-Qing Fan
Beijing Hospital

Lv-Tao Zeng
Beijing Hospital

Zhen-Xiang Gao
Beijing Hospital

Ji-Hong Hu
Beijing Hospital

Jian-Ping Cai
Beijing Hospital

Research

Keywords:

Posted Date: April 7th, 2020

DOI: https://doi.org/10.21203/rs.3.rs-21144/v1

Systemic RNA oxidation can be used as an index of clinical infection and prognosis in a *Vibrio parahaemolyticus* Challenge Rat Model

Ya-Ya Pian [1#], Jing-Jing Nie [1#], Chen-Chen Wang [2, 3], Qian Liu [3], Zhen Liu [2], Wei Zhang [4], Li-Qun Zhang [2], Qiu-geng Ou-Yang [3], Guo-Qing Fan [2] Lv-Tao Zeng [2], Zhen-Xiang Gao [1], Ji-Hong Hu [1*] and Jian-Ping Cai [2*]

[1] National Center for Clinical Laboratories, Beijing Hospital, National Center of Gerontology; Institute of Geriatric Medicine, Chinese Academy of Medical Sciences, Beijing 100730, China; [2] The Key Laboratory of Geriatrics, Beijing Institute of Geriatrics, Beijing Hospital, National Center of Gerontology, National Health Commission; Institute of Geriatric Medicine, Chinese Academy of Medical Sciences, Beijing 100730, China; [3] Department of Pharmacy, Wenzhou Medical University, Wenzhou 325035, China; [4] Department of Pathology, Beijing Hospital, National Center of Gerontology, Beijing 100730, China

[#]These authors contributed equally to this work.

*To whom all correspondence should be addressed. E-mail: caijp61@vip.sina.com and hujh68@126.com.

ABSTRACT

Background: More and more evidence supports the concept that RNA oxidation plays a substantial role in the progress of multiple diseases; however, only a few studies have reported RNA oxidation caused by microbial pathogens. Urinary 8-oxo-7,8-dihydroguanosine (8-oxo-Gsn) and 8-oxo-7,8-dihydro-2′-deoxyguanosine (8-oxo-dGsn), which are broadly used as indicators of oxidative damage of RNA and DNA, were analyzed in this study to determine which can be used as an index of clinical infection and prognosis in a *Vibrio parahaemolyticus* challenge rat model. In this study, twenty-four specific-pathogen-free (SPF) male SD rats were randomly divided into two groups: an infection group and a phosphate-buffered saline (PBS) control group. An LC-MS/MS-based system was established to determine the 8-oxo-dGsn and 8-oxo-Gsn contents of urine samples. The immunohistochemistry (IHC) was used to determine the 8-oxoguanine in nuclear DNA and in cellular RNA of different tissues of rats. Hematoxylin-eosin (H&E) stain was used to analyze intestinal inflammation. Sysmex XS-1000i hematology was used to analyze WBCs in blood. Luminex and ELISA were used to detect the level of inflammatory factors in serum. In addition, body temperatures, body weights, bacterial burden of *Vibrio parahaemolyticus* were also detected.

Results: The level of urinary and tissular 8-oxo-Gsn rather than 8-oxo-dGsn was significantly increased after infection with *V. parahaemolyticus* compared with PBS control. Stimultaneously, intestinal inflammation, the numbers of white blood cells (WBCs) and inflammatory factors (including CRP, IL-6, IL-1β, TNF-α, IL-10 and IL-

17A) were increased sharply. What is clinical significance is that the trend of urinary 8-oxo-Gsn was consistent with WBCs or inflammation. It is more important that the concentration of urinary 8-oxo-Gsn in the infection group was positively correlated with WBCs and inflammatory cytokines.

Conclusion: Our results demonstrated that 8-oxo-Gsn can be used as a more effective biomarker of clinical infection and prognosis compared with classic clinical indicators such as IL-6 and TNF-α.

Keywords: RNA oxidation; 8-oxo-Gsn; inflammation; *Vibrio parahaemolyticus*

Backgound

More and more evidence supports that RNA oxidation plays a substantial role in the progress of multiple diseases, such as Alzheimer's disease[1], diabetes [2] and aging [3], and plenty of studies have reported microbial pathogens can induce the increase of oxidative stress and inflammation[4-7]. However, only a few studies have reported RNA oxidation caused by microbial pathogens[8].

Vibrio parahaemolyticus, a Gram-negative halophilic bacterium that inhabits marine, estuarine and coastal waters around the world [9-11], is the main pathogen responsible for human acute gastroenteritis after consuming contaminated raw or undercooked seafood [12, 13]. Many gastroenteritis cases of *V. parahaemolyticus* have been reported worldwide, including Asia and the USA [9, 14], and clinical symptoms of *V. parahaemolyticus* include diarrhea, abdominal cramps, vomiting, headaches and a fever [15]. Owing to the clinical significance of *V. parahaemolyticus*, it was used as an infection model to study RNA oxidation in our research.

Reactive oxygen species (ROS) are constantly produced intracellularly under physiological conditions as a result of cellular metabolism and external conditions [16]. Persistently generated ROS can damage macromolecules, such as nucleic acids, protein and lipids, subsequently resulting in various diseases. Such nucleic acid oxidation plays crucial roles in the pathophysiology progress of various diseases [17]. 8-oxoguanine in nuclear DNA and in cellular RNA are the most widely used indicators of oxidative stress [18, 19], and many studies have shown 8-oxoguanine is a perfect marker for the detection of oxidative stress[20-23].

Urinary 8-oxo-Gsn and 8-oxo-dGsn, which are broadly used as indicators of oxidative damage of RNA and DNA, were analyzed in this study. An LC-MS/MS-based system was established to determine the 8-oxo-dGsn and 8-oxo-Gsn contents of urine samples. The immunohistochemistry (IHC) was used to determine the 8-oxoguanine in nuclear DNA and in cellular RNA of different tissues of rats. Hematoxylin-eosin (H&E) stain was used to analyze intestinal inflammation. Sysmex XS-1000i hematology was used to analyze WBCs in blood. Luminex and ELISA methods were used to detect the level of inflammatory factors in serum. We herein provide evidence that urinary 8-oxo-Gsn can be used as a more effective biomarker of clinical infection and prognosis compared with classic clinical indicators such as CRP or IL-6.

Results

RNA Oxidation Increased in Urine after Infection with *V. parahaemolyticus*

The level of 8-oxo-Gsn and 8-oxo-dGsn in urine samples was measured by the UHPLC-MS/MS method. Figure 1 showed the concentration of 8-oxo-Gsn and 8-oxo-dGsn in urine samples of SD rats (PBS control versus *V. parahaemolyticus*-infected). From Figure 1A, we can see that the level of urinary 8-oxo-Gsn in infection group was sharply increased from D1 to D5, peaking at D5 and gradually decreased thereafter, especially at D13, the level had almost returned to the pre-infection (D0). About the PBS control animals, the level of urinary 8-oxo-Gsn always kept a steady baseline. Creatinine (Cre) was used for normalizing the oxidized guanosine level. There was not statistically significant difference of 8-oxo-dGsn in urine at any time between these two groups, and the value was much lower than 8-oxo-Gsn (Figure 1B). In summary, our results showed that the level of urinary 8-oxo-Gsn other than 8-oxo-dGsn was dramatically increased after infection with *V. parahaemolyticus*.

RNA Oxidation Increased in Tissues after Infection with *V. parahaemolyticus*

Corresponding antibodies were used to detect 8-oxo-dGsn in nuclear DNA and 8-oxo-Gsn in cellular RNA of SI, spleen, colon and liver of SD rats challenged with *V. parahaemolyticus* at D0, D1, D5. To detect 8-oxo-Gsn in cellular RNA, immunostaining using antibodies against 8-oxoGsn was performed. The level of 8-oxo-Gsn in cellular RNA in SI and spleen was boosted gradually from D0 to D5, which was different from colon and liver, they peaked at D1 (Figure 2A). To detect 8-oxo-dGsn in nuclear DNA, antibodies against 8-oxo-dGsn were applied to tissue sections. From Figure 2B, we

can see that there was not statistically significant difference in SI, spleen or liver from beginning to end, but 8-oxo-dGsn in colon was boosted from D0 to D5 and peaked at D1. In a word, our results demonstrated that 8-oxo-Gsn in cellular RNA other than 8-oxo-dGsn in nuclear DNA maybe a systemic biomarker after infection with *V. parahaemolyticus*.

Inflammation Enhanced after SD Rats Challenged with *V. parahaemolyticus*

Inflammation was detected in colon of SD rats after challenge with this bacteria. H&E stain of the colon of the infected rats at D0, D1, D5, D9 and D18 was shown in Figure 3A. There was a bit lymphocytes infiltration under physiological conditions (D0), the red arrows showed the infiltration of lymphocytes in colon. However, lymphocytes infiltration increased quickly from D1 to D5, then gradually decreased from D5 to D18, especially dropping particularly low at D18 (back to almost physiological state).

We also counted the WBCs in blood, which was as low as PBS-treated control animals before infection but sharply increased from D1 to D5 and peaked at D5 before gradually decreased from D5 to D18. The WBCs remained at a very low level in PBS group animals. The body temperatures and body weights were also determined, yet there was no significant difference (supplementary Figures 1/2, respectively). The bacterial burden in stool gradually decreased, and no bacteria detected at D11, which was shown in supplementary Figure 3. No *V. parahaemolyticus* were observed in stool in PBS control animals, indicating that the animals were not contaminated. In summary, our results showed that inflammation was enhanced after SD rats were challenged with *V. parahaemolyticus*.

Upregulation of Inflammatory Cytokines in Serum Samples

In addition to the infiltration of lymphocytes and WBCs, the inflammatory cytokines were also detected in our research. Several significant inflammatory cytokines were tested in the serum samples, including IL-6, IL-10, TNFα, IL-1β, IL-17A and CRP. IL-6, IL-10, TNF-α, IL-1β and IL-17A were analyzed using the Luminex system, which were shown in Figures 4A to 4E. CRP was detected using the ELISA method, which was shown in Figure 4F. From Figure 4 we can see that inflammatory cytokines were dramatically increased from D1 to D5 after infection, peaking at D5 and gradually decreased from D5 to D18. As a PBS control, there was not statistically significant difference at any time in our study.

Correlation analysis of 8-oxo-Gsn with WBCs and inflammatory cytokines

The concentration of urinary 8-oxo-Gsn in the infection group was positively correlated with WBCs ($r=0.454$, $P<0.0001$) and inflammatory cytokines: CRP ($r=0.678$, $P<0.001$), IL-6 ($r=0.279$, $P<0.05$), IL-10 ($r=0.409$, $P<0.001$), TNF-α ($r=0.457$, $P<0.001$), IL-1β ($r=0.604$, $P<0.001$) and IL-17A ($r=0.543$, $P<0.001$). The predictive value of 8-oxo-Gsn, WBCs and inflammatory cytokines was assessed by the ROC curve. From Figure 5, we can see that the area under ROC curve of urinary 8-oxo-Gsn, WBCs, CRP, IL-6, IL-10, TNF-α, IL-1β and IL-17A was 0.778 (95% CI, 0.629-0.926, $P<0.001$), 0.883 (95% CI, 0.798-0.967, $P<0.001$), 0.972 (95% CI, 0.935-1.009, $P<0.001$), 0.739 (95% CI, 0.605-0.874, $P<0.001$), 0.912 (95% CI, 0.831-0.994, $P<0.001$), 0.942 (95% CI, 0.869-1.014, $P<0.001$), 0.953 (95% CI, 0.908-0.997, $P<0.001$), and 0.919 (95% CI, 0.855-0.983, $P<0.001$), respectively. These statistic analysis confirmed that 8-oxo-Gsn

was closely related with inflammation.

Discussion

The present study showed that RNA oxidation dramatically elevated in urine and tissues of rats after infection with *V. parahaemolyticus*. RNA oxidation, which plays a substantial role in the progress of multiple diseases, have studied in many fields, such as diabetes and aging, but only a few studies have reported in microbial pathogens. For this purpose, we studied RNA oxidation caused by microbial pathogens.

As by-products of oxidative stress, 8-oxo-Gsn other than 8-oxo-dGsn has shown increased in urine and partial tissues after challenge with *S*. Enteritidis[8]. However, it doesn't compare with other classic clinical indicators such as CRP or IL-6, and also doesn't prove whether other pathogens can cause RNA oxidation. Another important reason for this study is we want to compare RNA oxidation with other classic clinical indicators such as CRP or IL-6. For this purpose, we choose an intestinal pathogenic bacteria-*V. parahaemolyticus* to test the correlation of RNA oxidation and inflammation.

While several animal models have been developed for the study of oxidative stress, such as mice, rabbits and piglets, we select SD rats for animal model because of the large volume of urine they produced. Our results showed that the level of 8-oxo-Gsn other than 8-oxo-dGsn in urine was sharply increased from D0 to D5, peaking at D5 and gradually decreased until D18. The inflammatory indicators we tested including intestinal inflammation, WBCs and inflammatory cytokines were both increased from D0 to D5, peaking at D5 and gradually decreased until D18. What is more importantly is the trend of urinary 8-oxo-Gsn was consistent with WBCs and inflammation. It has very important clinical significance: 8-oxo-Gsn is better than inflammatory cytokines in

clinical, because it only needs urine samples. We also detected 8-oxo-Gsn and 8-oxo-dGsn in tissues, including small intestine, liver, spleen and colon. Consistent with the urine results, 8-oxo-Gsn was markedly increased in liver, spleen, small intestine and colon from D0 to D5 too, but however, D1 was higher than D5 in liver and colon, maybe there are some different mechanisms in these tissues. 8-oxo-dGsn had no changes in tissues except for the colon. These results suggested that *V. parahaemolyticus* can lead to a systemic RNA oxidation in our study.

What is the mechanism of the increase of RNA oxidation in urine and tissues? We think one possible explanation is that ROS produced by *V. parahaemolyticus* flooded the bloodstream and diffused into the tissues in forms such as superoxide ($\cdot O_2^-$), hydrogen peroxide (H_2O_2) and hydroxyl radical ($\cdot OH$). Another possible interpretation is that bacteria may have been carried by phygocytes to colonize the liver and spleen, thus inducing RNA oxidation; however, we did not detect any bacteria in liver or spleen. So another explanation maybe toxins, such as Shiga toxins and Shiga-like toxins (Stx1 or Stx2 with variants), especially Stx2, can reach many organs and induce oxidative stress [24]. We believe toxins produced by *V. parahaemolyticus* may be responsible for the RNA oxidation observed in our study, but is the direction of our future research. In a word, our results showed that 8-oxo-Gsn can be used as a more effective biomarker of clinical infection and prognosis compared with classic clinical indicators.

Conclusion

This study found that SD rats were infected with *V. parahaemolyticus* can induce the increasing of RNA oxidation and inflammation at the same time. Through the LC-MS/MS-based system and IHC we proved the level of urinary and tissular 8-oxo-Gsn rather than 8-oxo-dGsn was significantly elevated infection with *V. parahaemolyticus*. Stimultaneously, white blood cells (WBCs), intestinal inflammation and inflammatory factors were increased sharply. What is more clinical significance is that the trend of urinary 8-oxo-Gsn was consistent with WBCs or inflammation. In a word, our results demonstrated that 8-oxo-Gsn can be used as a more effective biomarker of clinical infection and prognosis compared with classic clinical indicators.

Materials and Methods

Chemicals and Experimental Reagents

High-performance liquid chromatography (HPLC)-grade solvents and ammonium acetate were purchased from Merk (Darmstadt, Germany) and Thermo Fisher Scientific (St, Leon-Rot, Germany), respectively. 8-oxo-Gsn (>98% purity), 8-oxo-dGsn (>98% purity) and isotope internal standard [$^{15}N_5$] 8-oxo-dGsn were purchased from Cambridge Isotope Laboratories (Andover, MA, USA). [$^{13}C_1$, $^{15}N_2$] 8-oxo-Gsn was customized by Toronto Research Chemicals (Ontario, Canada). RNase A and DNase I were purchased from TaKaRa Biotechnology Co., Ltd. (Dalian, China). 15A3 and N45.1 mAb were obtained from Abcam (Cambridge, UK). The H&E Stain kit and DAB Peroxidase (HRP) Substrate kit were purchased from Beijing Zhongshan Jinqiao Biotechnology Co., Ltd. (Beijing, China). MILLIPLEX MAP Rat Cytokine/Chemokine Kit was purchased from EMD Millipore Corporation (Billerica, MA, USA). The Luminex 200 system was obtained from Luminex Corporation (Austin, TX, USA). The Rat CRP ELISA kit was come from Immunology Consultants Laboratory, Inc. (ICL, Portland, USA). Water used for the analysis was deionized at 18.2 MΩ.

Bacterial Strains and Culture Conditions

V. parahaemolyticus (ATCC 17802) used in this study was come from American Type Culture Collection (ATCC, Rockville, MD, USA), which was recovered from the frozen conditions and streaked onto blood agar plates (Columbia agar supplemented with 5% sheep blood, bioMérieux) to obtain some single colonies. A single colony was inoculated in Tryptone Soya Broth (TSB) supplemented with 3% NaCl liquid medium

and shaken sharply at 35±2 °C, and then 1% was transferred and cultured under the same conditions. The bacteria were harvested at the stationary growth phase for experimentation after being washed two times with sterile PBS.

Animals and Treatments

Twenty-four 3-week-old SPF male SD rats (80-90 g) were purchased from Beijing Vital River Laboratory Animal Technology Co., Ltd. These animals were housed in a temperature-controlled SPF chamber (24±2 °C) with a 12-h light/dark cycle for about one week to acclimate them to the environment. All animal operations were performed in a biosafety level 3 (BSL3) facility and were approved by the local ethics committee. These animals were divided into two groups: an infection group and a PBS control group. The infection group were challenged with 10^{10} CFU bacteria per rat via gastric gavage, while the control group were orally administered sterile PBS. All animals were fasted for 16 h before treatments. Common clinical symptoms, including body weights, body temperatures, bacterial burden, WBCs, intestinal inflammation, inflammatory cytokines, urinary and tissular 8-oxoguanine were both analyzed. Urine samples were collected using the manual bladder palpation method and stored at -80 °C. For tissue acquisition, three rats each were killed at D1, D5, D9 and D18 and immediately placed into 10% formalin-fixed liquid for the assessment of oxidative damage of DNA and RNA. To assess the concentration of WBCs in blood, samples were anticoagulated by K_3EDTA and subjected to a Sysmex XS-1000i hematology analysis (Sysmex Corp., Kobe, Japan) every four days. Serum samples were collected without anticoagulant and stored at -80 °C until analysis.

296 **Bacterial Burden in Stool**

297 Bacterial burden of *V. parahaemolyticus* in stool were counted on chromogenic
298 medium (CHROMagar Microbiology, Paris, France). The bacteria appeared as mauve
299 colonies in this selective solid medium. Quantitative analysis was applied to measure
300 bacterial burden. In brief, stool samples were collected and weighed before grinding
301 using a Pro200 rotor-stator homogeniser (PRO Scientific Inc., Oxford, CT USA). Stool
302 samples were then centrifuged gently and diluted in PBS and plated onto plate. The
303 mauve colonies were recorded as *V. parahaemolyticus*. All operations were performed
304 in a BSL3 facility.

305 **Chromatographic and Mass Spectrometric Analyses**

306 All samples were separated using an Agilent 1290 Infinity ultra-HPLC (UHPLC)
307 instrument (Agilent1290; California, USA). The chromatographic separation was
308 performed on an Agilent C18 (3 μm, 3.00×100 mm) column at 35 °C. The mobile phase
309 consisted of mobile phase A (5 mM ammonium acetate with 0.1% formic acid) and
310 mobile phase B (methanol with 0.1% formic acid). The flow rate was 0.4 mL/min. To
311 reduce the loss of the sample solution, the sample room temperature was kept at 4 °C.
312 Early- and late-eluting components were discarded in order to ensure the data had no
313 interference. The UHPLC conditions are summarized in supplementary Table 1. The
314 UHPLC tandem mass spectrometry (UHPLC-MS/MS) instrument was equipped with
315 an Agilent triple-quadrupole mass spectrometer with a JetStream ESI source and
316 IFunnel (Agilent 6490; California, USA). The detection was performed in the positive-
317 ion detection mode, and multiple reaction mode (MRM) was monitored for the

quantitative analysis. The optimum nitrogen value for the nebulizer was 30 psi, and the ESI needle voltage was 2000 V. The temperature of the dry gas and sheath gas was set at 200 and 400 °C, respectively, while the flow rate was 16 and 12 L/min, respectively. The low- and high-pressure RF (radio frequency) was 50 and 120 V, respectively. The optimized parameters are summarized in supplementary Tables 2 and 3.

Detection DNA and RNA Oxidation Level in Urine Samples

Urine samples frozen at -80 °C were thawed on ice and centrifuged at 7500 *g* for 5 min at 4 °C. To each 200 μL aliquot of the supernatant, 200 μL of working solution (70% methanol, 30% water with 0.1% formic acid, 10 mM ammonium acetate, pH 3.7) was added, followed by 10 μL of 2 corresponding internal standards (240 pg/μL). The mixtures were then incubated at 35±2 °C for 10 min and centrifuged at 12,000 *g* for 15 min at 4 °C. Finally, 100 μL of the supernatant was subjected to UHPLC-MS/MS. Because of variations in the urinary volume and significant differences in the renal glomerular function, the concentration of analytes was adjusted by the creatinine level [25-27], which was determined using an automatic biochemical analyzer 7600 series (Hitachi High Technologies, Tokyo, Japan).

Tissue Processing and Histopathologic Examinations

Tissue samples, including the small intestine (SI), colon, spleen and liver were dissected and placed into 10% formalin-fixed liquid for IHC and H&E analysis. Sample sections were stained with H&E reagents according to the routine procedures. In brief, tissues were dehydrated in a graded series of alcohol washes, embedded in paraffin,

sectioned into 4-μm slices, followed by H&E stain for a microscopic examination. All sections were photographed using a 100× light microscope (Nikon, Tokyo, Japan).

IHC

IHC was performed using labeled 4-μm-thick sections of formalin-fixed and paraffin-blocked sections. All sections were dewaxed using xylene and gradually dehydrated with gradient ethanol and washed with PBS. Antigen retrieval was performed by microwaveing at 95 °C for 40 min with buffer solution of citrate salts. For the detection of 8-oxo-dGsn in nuclear DNA, sections were treated with 5 mg/mL RNase A overnight at 37 °C to eliminate cellular RNA. To detect 8-oxo-Gsn in cellular RNA, the sections were treated with DNase I overnight at 37 °C to remove nuclear DNA. After treatment with 3% H_2O_2 for 20 min and blocking with 10% normal goat serum for 30 min, the primary monoclonal antibodies 15A3 to detect 8-oxo-Gsn in cellular RNA and N45.1 to detect 8-oxo-dGsn in nuclear DNA were added to the tissue sections at 37 °C for 2 h. The sections were then incubated with a secondary antibody for 30 min at room temperature. All sections were treated with the HRP DAB Detection System (ZSGB BIO) for 20 min and visualized using a DAB kit (ZSGB-BIO).

Inflammatory Cytokines detected by Luminex and ELISA

The level of inflammatory cytokines was detected by the MILLIPLEX MAP Rat Cytokine/Chemokine Kit and Luminex 200 system (Luminex Corporation, Austin, TX, USA). The procedures were according to the protocol in the kit. All reagents were to be balanced to room temperature before detection. First, 200 μL assay buffer was added to each well of a 96-well plate and shaken on a plate shaker for 10 min at room

temperature. Discarded assay buffer, added 25 μL standards buffer, 25 μL control buffer or 25 μL assay buffer to the 96-well plate, then 25 μL serum matrix solution and 25 μL serum, following 25 μL beads. The plate was sealed and incubated with agitation for 2 h at room temperature. Each well was then washed twice using 200 μL wash buffer. Detection antibodies (25 μL) were added and incubated with agitation for 1 h at room temperature, after which 25 μL Streptavidin-Phycoerythrin was added and incubated for 30 min at room temperature. Each well was washed twice using 200 μL wash buffer, and then 125 μL sheath fluid was added and shaken for 5 min to read on a Luminex 200 system.

The level of CRP was determined using a Rat CRP ELISA kit. The procedures were according to the protocol in the kit. All reagents were to be balanced to room temperature before testing. First, the serum samples were diluted 120000 times and then added to a 96-well plate. The standard concentration were 0, 6.25, 12.5, 25, 50, 100 and 200 ng/mL. The plate was sealed and stored for 10 min at room temperature, followed by washing 5 times using 200 μL wash buffer. Next, 100 μL Enzyme-Antibody Conjugate was added, followed by incubation in dark for 10 min at room temperature and then washing 5 times using 200 μL wash buffer with 100 μL TMB substrate solution added. The plate was then incubated in dark at room temperature for 5 min before adding 100 μL stop solution, at which point the OD_{450} value was determined, and the standard curve was drawn to calculate the CRP concentration.

Statistical analysis

Unless otherwise specified, all of the data in this research are expressed as the

mean±standard error of the mean (SEM). Differences between the PBS control and the infection group were analyzed using an unpaired two-tailed Student's t-test or a one-way analysis of variance. For all tests, a P value of <0.05 was considered the threshold for significance. All statistical analysis in this study were performed with the GraphPad Prism 8.0 software program (GraphPad Software Inc, San Diego, CA, USA). For correlation analysis of 8-oxo-Gsn with others, the receiver operator characteristic (ROC) curve was accepted with the SPSS 20 software (IBM Corporation, Armonk, NY, USA).

Abbreviations

SPF: specific-pathogen-free; 8-oxo-Gsn: 8-oxo-7,8-dihydroguanosine; 8-oxo-dGsn: 8-oxo-7,8-dihydro-2′-deoxyguanosine; IHC: immunohistochemistry; H&E: hematoxylin-eosin; PBS: phosphate-buffered saline; *V. parahaemolyticus*: *Vibrio parahaemolyticus*; WBCs: white blood cells; ROS: reactive oxygen species; Cre: creatinine; SI: small intestine; ATCC: American Type Culture Collection; TSB: Tryptone Soya Broth; BSL3: biosafety level 3; MRM: multiple reaction mode; SEM: standard error of the mean; ROC: receiver operator characteristic.

Authors' contributions

Ya-ya Pian, Ji-hong Hu and Jian-ping Cai designed the study and wrote the manuscript. Ya-ya Pian and Jing-jing Nie performed the experiments and analyzed the data. Chen-chen Wang, Qian Liu and Zhen Liu perfromed the MS work. Qiu-geng Ou-Yang, Guo-qing fan, Li-qun Zhang and Lv-tao Zeng did the IHC job. Wei Zhang and Zhen-xiang Gao performed the experiments.

Funding

This work was supported by the CAMS Innovation Fund for Medical Sciences (No. 2018-I2M-1-002), National Key R&D Program of China (2018YFC2000300), National Natural Science Foundation of China (No. 81571058), Beijing Hospital Doctor Foundation Project (bj-2018-027), Beijing Gold-Bridge Project (ZZ19059) and Beijing Dongcheng District Outstanding Talent Funding Project (2019DCT-M-11).

Availability of data and materials

All data generated or analyzed during this study are included in this published article.

Ethics approval and consent to participate

The animal experiments were approved by the local ethics committee.

Consent for publication

Not applicable.

Competing interests

The authors declare that they have no competing interests.

Acknowledgments

We are grateful to the members of the Institute of Geriatrics of the Ministry of Health for their advice and assistance.

References

1. Song X-N, Zhang L-Q, Liu D-G, Lin J, Zheng J-D, Dai D-P, et al. Oxidative Damage to RNA and Expression Patterns of MTH1 in the Hippocampi of Senescence-Accelerated SAMP8 Mice and Alzheimer's Disease Patients. Neurochemical Research 2011; 36:1558-65.

2. Wang WX, Luo SB, Xia MM, Mao YH, Zhou XY, Jiang P, et al. Analysis of the oxidative damage of DNA, RNA, and their metabolites induced by hyperglycemia and related nephropathy in Sprague Dawley rats. Free Radic Res 2015; 49:1199-209.

3. Gan W, Liu XL, Yu T, Zou YG, Li TT, Wang S, et al. Urinary 8-oxo-7,8-dihydroguanosine as a Potential Biomarker of Aging. Front Aging Neurosci 2018; 10:34.

4. Ling PR, Smith RJ, Bistrian BR. Acute effects of hyperglycemia and hyperinsulinemia on hepatic oxidative stress and the systemic inflammatory response in rats. Crit Care Med 2007; 35:555-60.

5. Hardbower DM, de Sablet T, Chaturvedi R, Wilson KT. Chronic inflammation and oxidative stress: the smoking gun for Helicobacter pylori-induced gastric cancer? Gut Microbes 2013; 4:475-81.

6. Ding SZ, Minohara Y, Fan XJ, Wang J, Reyes VE, Patel J, et al. Helicobacter pylori infection induces oxidative stress and programmed cell death in human gastric epithelial cells. Infect Immun 2007; 75:4030-9.

7. Patel B, Kumar P, Banerjee R, Basu M, Pal A, Samanta M, et al. Lactobacillus acidophilus attenuates Aeromonas hydrophila induced cytotoxicity in catla thymus macrophages by modulating oxidative stress and inflammation. Mol Immunol 2016; 75:69-83.

8. Hu JH, Nie JJ, Gao ZX, Weng QH, Wang ZH, Li CB, et al. Oxidative DNA and RNA damage and their prognostic values during Salmonella enteritidis-induced intestinal infection in rats. Free Radic Res 2018; 52:961-9.

9. Su YC, Liu C. Vibrio parahaemolyticus: a concern of seafood safety. Food Microbiol 2007; 24:549-58.

10. Zhang L, Orth K. Virulence determinants for Vibrio parahaemolyticus infection. Curr Opin Microbiol 2013; 16:70-7.

11. Jung SW. A foodborne outbreak of gastroenteritis caused by Vibrio parahaemolyticus associated with cross-contamination from squid in Korea. Epidemiol Health 2018; 40:e2018056.

12. Kawatsu K, Ishibashi M, Tsukamoto T. Development and evaluation of a rapid, simple, and sensitive immunochromatographic assay to detect thermostable direct hemolysin produced by Vibrio parahaemolyticus in enrichment cultures of stool specimens. J Clin Microbiol 2006; 44:1821-7.

13. Newton A, Kendall M, Vugia DJ, Henao OL, Mahon BE. Increasing rates of vibriosis in the United States, 1996-2010: review of surveillance data from 2 systems. Clin Infect Dis 2012; 54 Suppl 5:S391-5.

14. Daniels NA ML, Bishop R, Altekruse S, Ray B, Hammond RM, Thompson S, Wilson S, Bean NH, Griffin PM, Slutsker L. Vibrio parahaemolyticus Infections in the United States, 1973–1998. J Infect Dis 2000; 181:1661-6.

15. William H Barker J, MD. and Eugene J. Gangarosa, MD. Food poisoning due to Vibrio parahaemolyticus. Annu Rev Med 1974; 25:75-81.

16. Jabs T. Reactive oxygen intermediates as mediators ofprogrammed cell death in plants and animals. Biochem Pharmacol 1999; 57:231-45.

17. Poulsen HE, Specht E, Broedbaek K, Henriksen T, Ellervik C, Mandrup-Poulsen T, et al. RNA modifications by oxidation: a novel disease mechanism? Free Radic Biol Med 2012; 52:1353-61.

18. Haghdoost S, Sjolander L, Czene S, Harms-Ringdahl M. The nucleotide pool is a significant target

for oxidative stress. Free Radic Biol Med 2006; 41:620-6.

19. Li Z, Wu J, Deleo CJ. RNA damage and surveillance under oxidative stress. IUBMB Life 2006; 58:581-8.

20. Gan W, Nie B, Shi F, Xu XM, Qian JC, Takagi Y, et al. Age-dependent increases in the oxidative damage of DNA, RNA, and their metabolites in normal and senescence-accelerated mice analyzed by LC-MS/MS: urinary 8-oxoguanosine as a novel biomarker of aging. Free Radic Biol Med 2012; 52:1700-7.

21. Nie B, Gan W, Shi F, Hu GX, Chen LG, Hayakawa H, et al. Age-dependent accumulation of 8-oxoguanine in the DNA and RNA in various rat tissues. Oxid Med Cell Longev 2013; 2013:303181.

22. Hu XX, Lan T, Chen Z, Yang CC, Tang PF, Yuan LJ, et al. A rapid and sensitive UHPLC-MS/MS assay for the determination of trelagliptin in rat plasma and its application to a pharmacokinetic study. J Chromatogr B Analyt Technol Biomed Life Sci 2016; 1033-1034:166-71.

23. Mao YH, Xu LN, Weng QH, Li XY, Zhao B, Nie JJ, et al. The Ratio of Plasma and Urinary 8-oxo-Gsn Could Be a Novel Evaluation Index for Patients with Chronic Kidney Disease. Oxid Med Cell Longev 2018; 2018:4237812.

24. !!! INVALID CITATION !!! [24,25].

25. Lee KF, Chung WY, Benzie IF. Urine 8-oxo-7,8-dihydro-2'-deoxyguanosine (8-oxodG), a specific marker of oxidative stress, using direct, isocratic LC-MS/MS: Method evaluation and application in study of biological variation in healthy adults. Clin Chim Acta 2010; 411:416-22.

26. Grew IS, Cejvanovic V, Broedbaek K, Henriksen T, Petersen M, Andersen JT, et al. Diurnal variation of urinary markers of nucleic acid oxidation. Scand J Clin Lab Invest 2014; 74:336-43.

27. To-Figueras J SM, Otero R, Barrot C, Santiago-Silva M, Rodamilans M, Herrero C, Grimalt J,

511 Sunyer J. Metabolism of hexachlorobenzene in humans: association between serum levels and urinary
512 metabolites in a highly exposed population. Environmental health perspectives. Environmental health
513 perspectives 1997; 105:78-83.
514
515

FIGURE LEGENDS

Figure 1. The level of 8-oxo-Gsn was boosted in urine of SD rats after challenge with *V. parahaemolyticus*. (A) and (B) indicated the concentration of 8-oxo-Gsn and 8-oxo-dGsn in urine increased with the passage of time by UHPLC-MS/MS, respectively. Creatinine (Cre) was used to normalize the oxidized guanosine level. All results are expressed as the mean±SEM. Statistical difference determined by the t-test. ***p*<0.01, *****p*<0.0001.

Figure 2. IHC determination for 8-oxo-dGsn in nuclear DNA and 8-oxo-Gsn in cellular RNA from tissues of rats. IHC stain for 8-oxo-Gsn in cellular RNA (A) and 8-oxo-dGsn in nuclear DNA (B) in small intestine (SI), spleen, colon and liver of SD rats at D0, D1, D5, respectively. All results are expressed as the mean±SEM. Significance determined using the t-test. **p*<0.05, ***p*<0.01, ****p*<0.001, *****p*<0.0001.

Figure 3. Inflammation heightened after infection with *V. parahaemolyticus*. (A) H&E stain of the colon of SD rats challenged with *V. parahaemolyticus* at D0, D1, D5, D9 and D18. The red arrows indicate the infiltration of lymphocytes in colon. Images were taken at ×100 magnification, except for the ×400 magnification zoomed-in local view at D5. (B) WBCs of SD rats with and without *V. parahaemolyticus* infection at D0, D1, D5, D9, D13 and D18. All results are expressed as the mean±SEM. Significance determined using the t-test. **p*<0.05, ***p*<0.01, *****p*<0.0001.

Figure 4. The concentration of inflammatory cytokines was increased after infection with *V. parahaemolyticus*. Luminex and ELISA were used to detect the concentration of IL-6, IL-10, TNF-α, IL-1β and IL-17A (A to E) and CRP (F), respectively. All results are expressed as the mean±SEM. Significance determined using the t-test. **p*<0.05, ***p*<0.01, ****p*<0.001, *****p*<0.0001.

Figure 5. The area under receiver operator characteristic (ROC) curve of 8-oxo-Gsn, WBCs and inflammatory cytokines including CRP, IL-6, IL-10, TNF-α, IL-1β and IL-17A for assessing the infection status.

FIGUREs

Figure 1

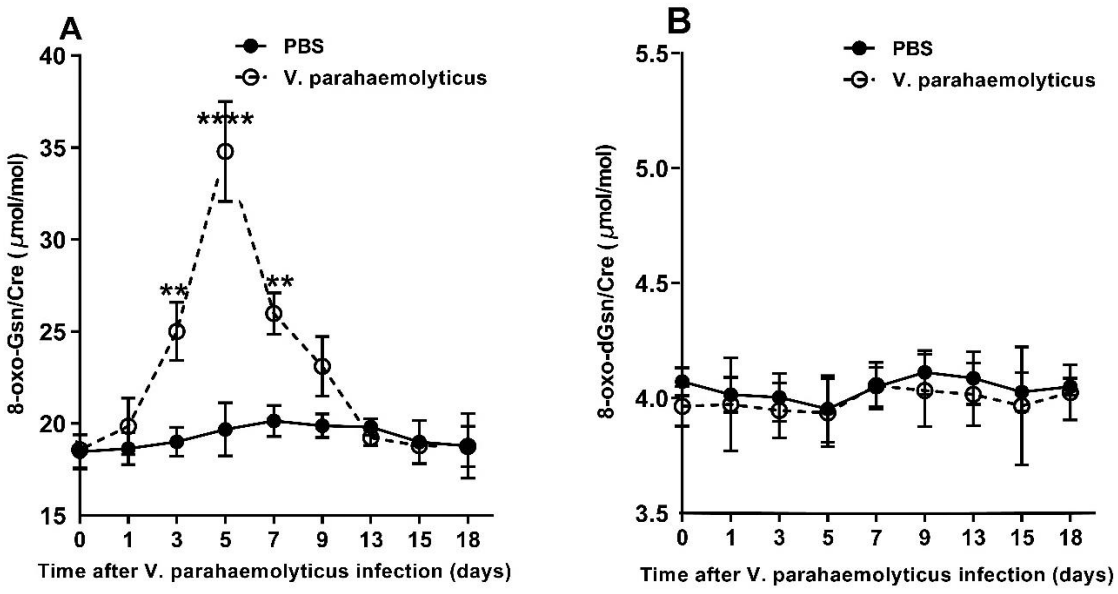

Figure 2

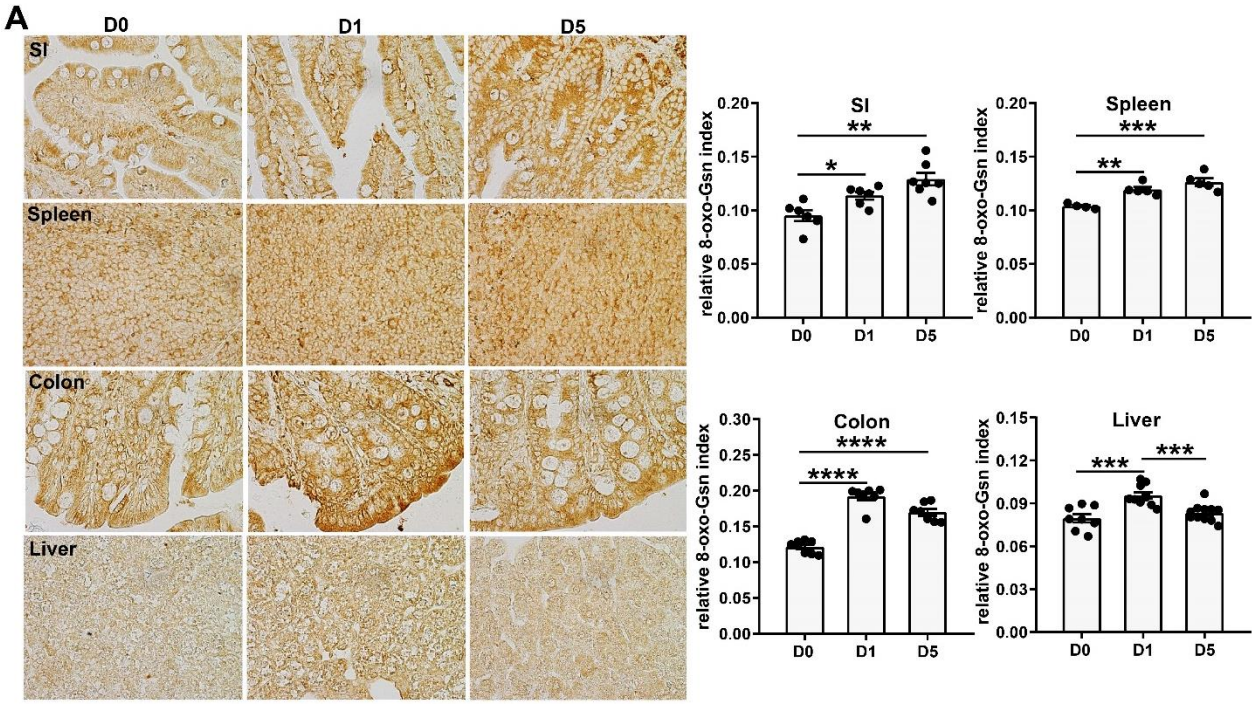
A
D0
D1
D5
SI
Spleen
Colon
Liver
relative 8-oxo-Gsn index
SI
Spleen
Colon
Liver
**
*
***
**
****
****
***
***
0.00
0.05
0.10
0.15
0.20
0.25
0.30
0.03
0.06
0.09
0.12

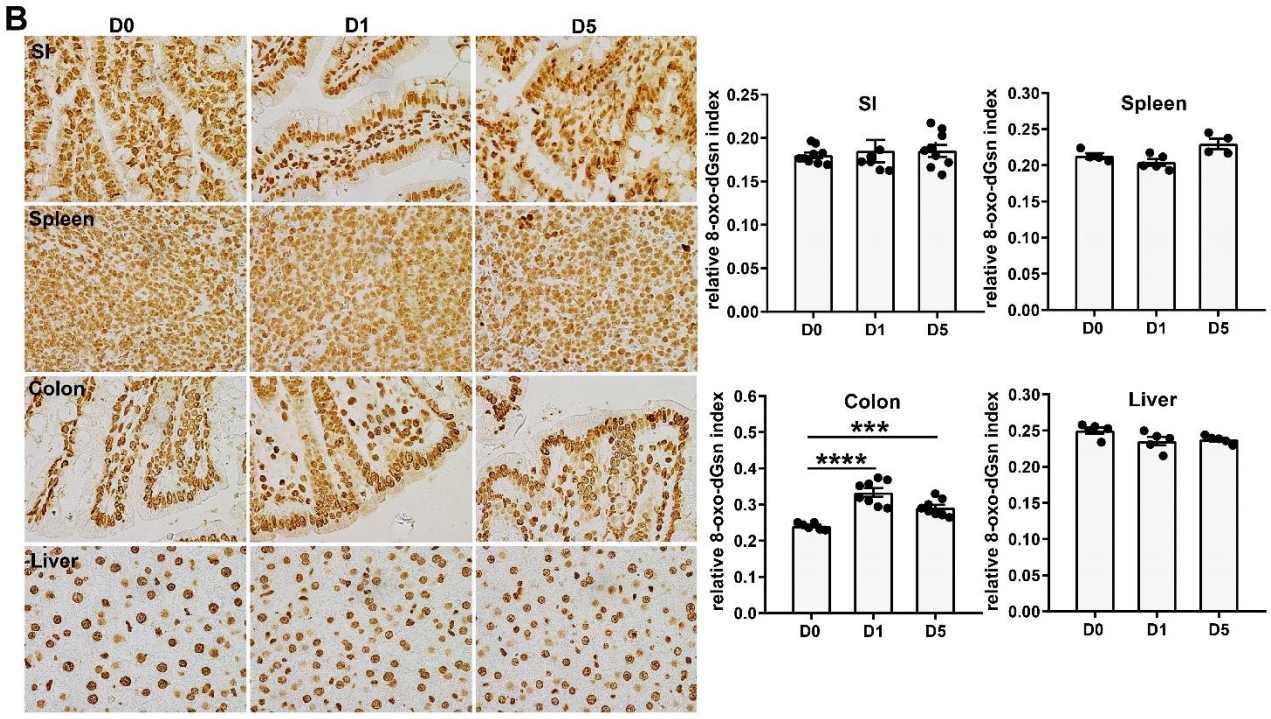
B
D0
D1
D5
SI
Spleen
Colon
Liver
relative 8-oxo-dGsn index
SI
Spleen
Colon
Liver
***
****
0.0
0.1
0.2
0.3
0.4
0.5
0.6
0.00
0.05
0.10
0.15
0.20
0.25
0.30

582 **Figure 3**

583

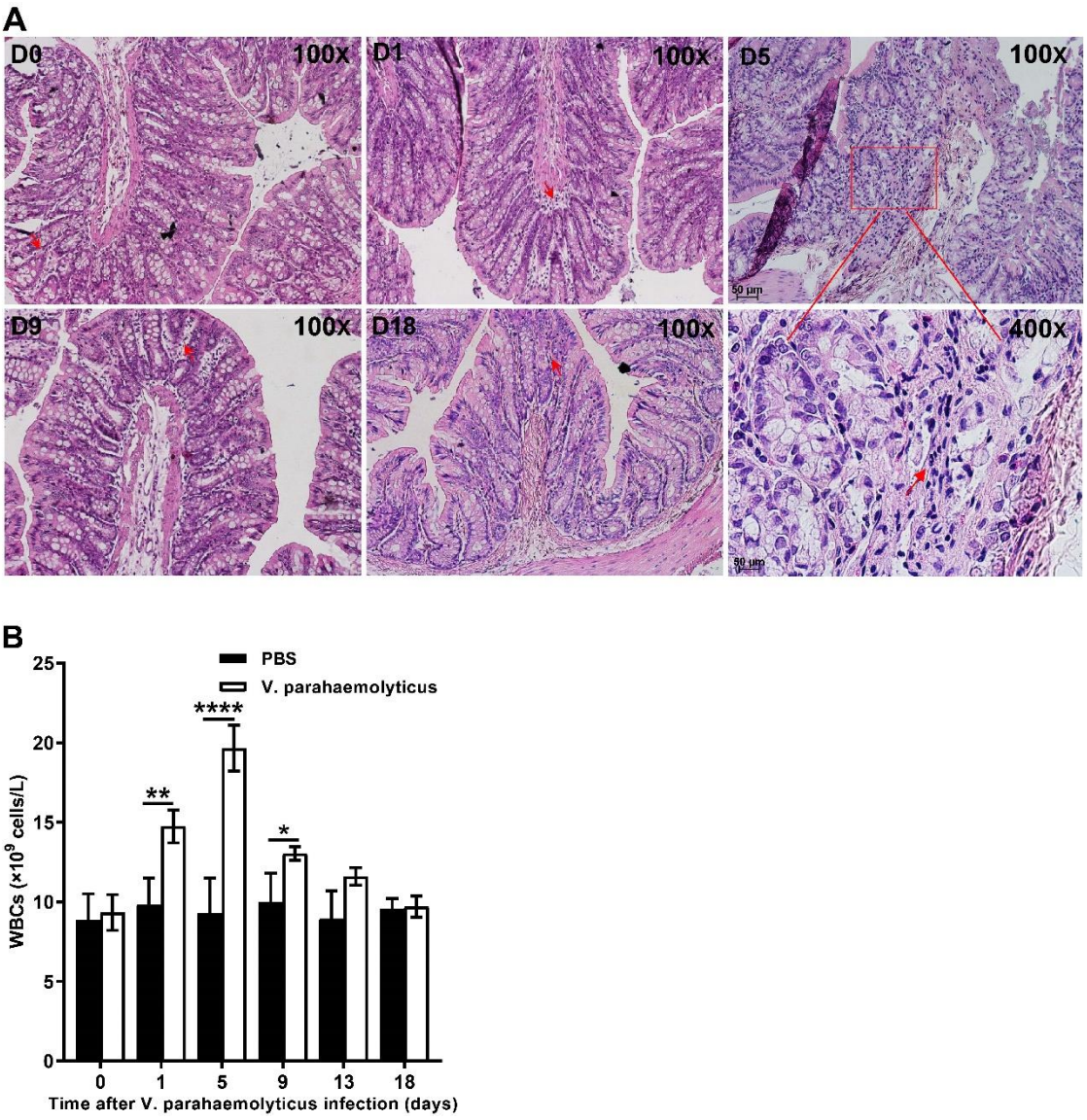

584

585

586

587

588

589

590

591 **Figure 4**

592

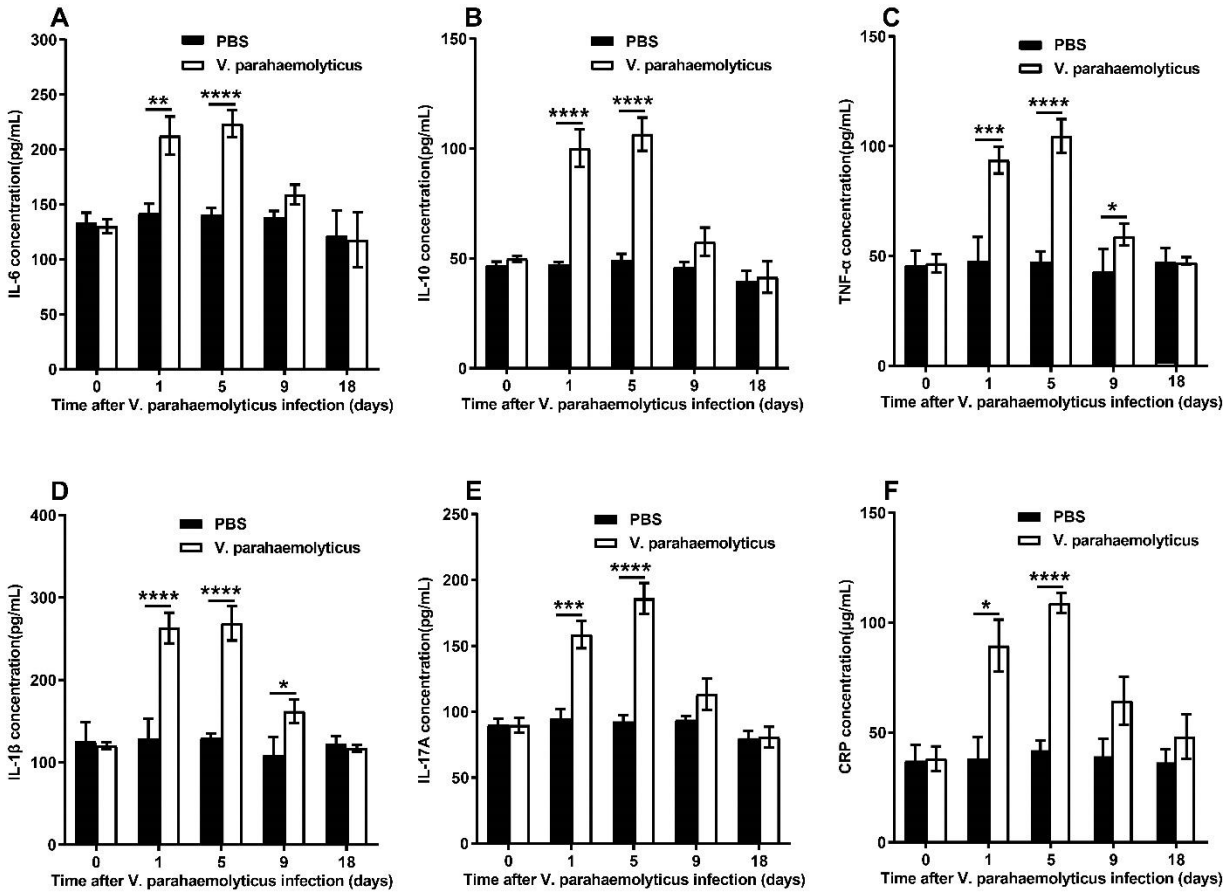

593

594

595

596

597

598

599

600

601

602

603 **Figure 5**

604

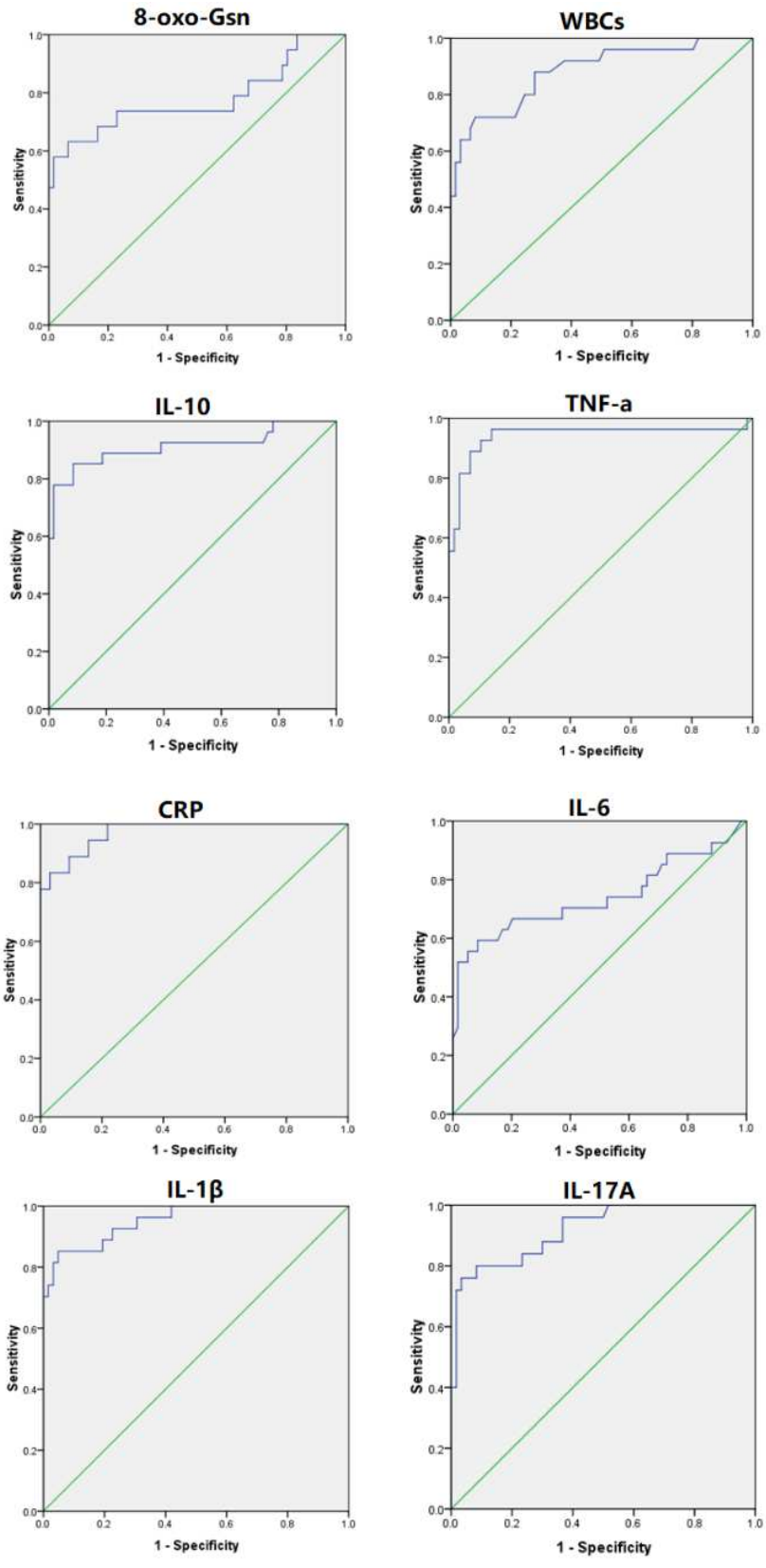

605

606

607 **Supplementary Materials**

608 **FIGURES**

609

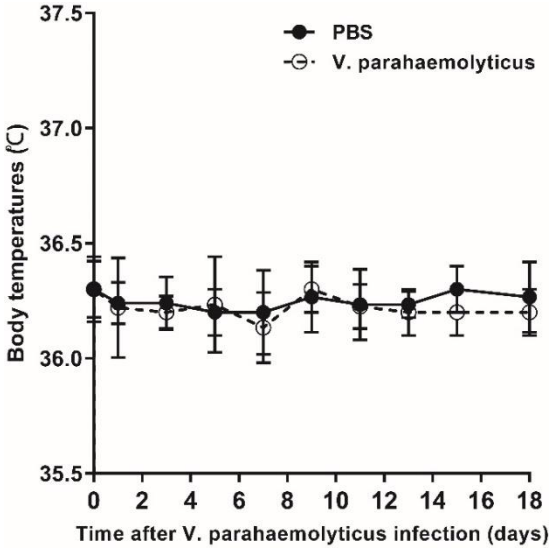

610

611 **Supplementary Figure 1.** Dynamic changes of body temperatures after SD rats were

612 challenged with *V. parahaemolyticus*. All rats were taken body temperatures every two

613 days.

614

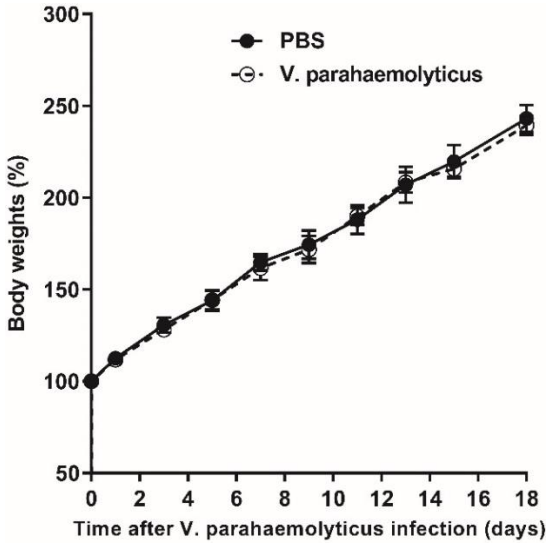

615

616 **Supplementary Figure 2.** Dynamic changes of body weights after SD rats were

617 challenged with *V. parahaemolyticus*. All rats were taken body weights every two days.

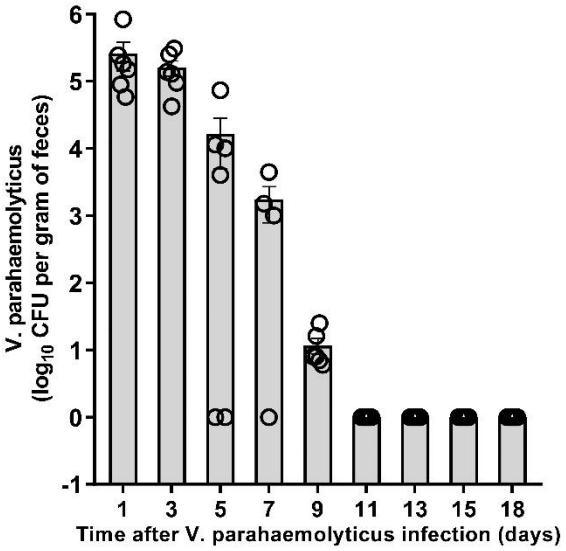

Supplementary Figure 3. Dynamic changes of bacterial burden per gram of stool after SD rats were challenged with *V. parahaemolyticus*. The bacteria counts in the *V. parahaemolyticus*-infected group was determined every two days.

TABLES

Table 1. LC conditions for urine samples

Sample	Temperature	Flow rate	The percentage of mobile phase A in relation to time				
			90%-70%	70%-2%	2%-2%	2%-90%	90%-90%
urine	35 °C	0.4 mL/min	0-3 min	3-4 min	4-5 min	5-5.01min	5.01-7min

Table 2. Conditions for different compounds in urine samples

sample	Compounds	MRM transitions for quantifier	Collision energy	MRM transitions for qualifier	Collision energy	Internal standard Mass pairs	Collision energy	Cell accelerator voltage
urine	8-oxo-dGsn	*m/z* 284-168	10 eV	m/z 284-140	32 eV	*m/z* 289-173	10 eV	3
	8-oxo-Gsn	*m/z* 300-168	14 eV	m/z 300-140	38 eV	*m/z* 303-171	12 eV	3

Table 3. MASS Conditions for urine samples

Type of sample	Gas temperature	Gas flow	Sheath gas temperature	Sheath gas flow	Nebulizer	Capillary	Nozzle voltage	High pressure RF	Low pressure RF
urine	200 °C	16 L/min	400 °C	12 L/min	30 psi	2000 V	0	120 V	50 V

Figures

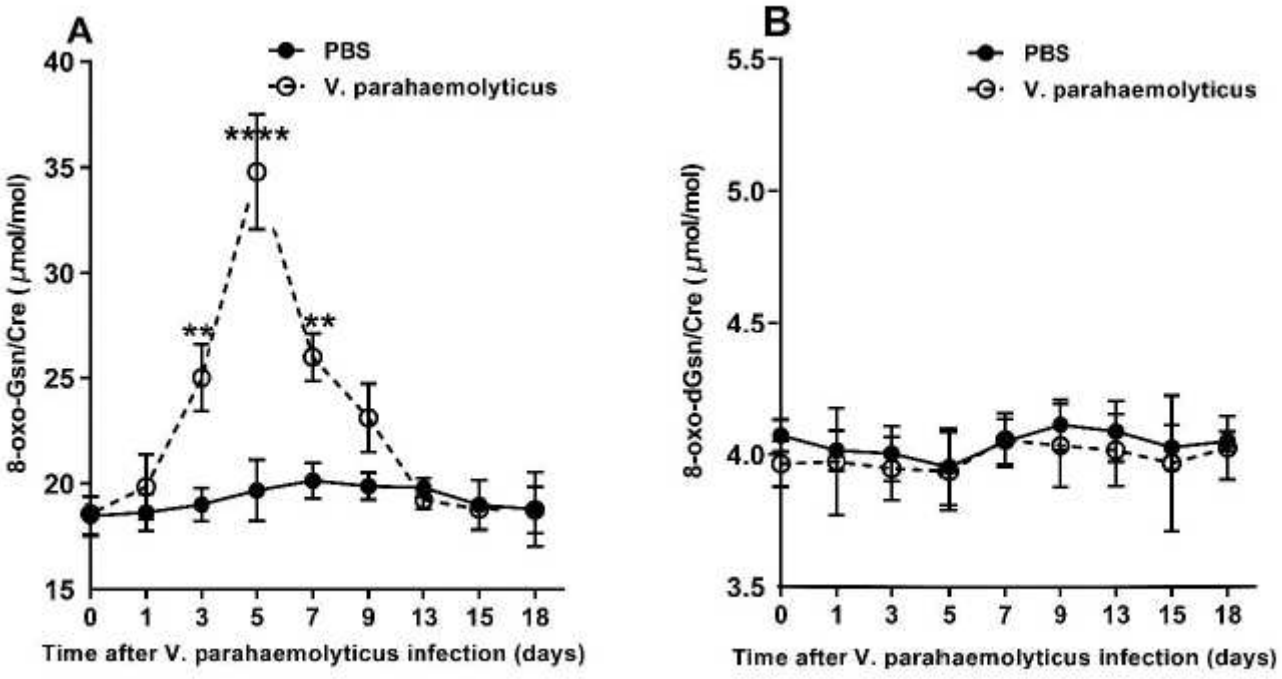

Figure 1

The level of 8-oxo-Gsn was boosted in urine of SD rats after challenge with V. parahaemolyticus. (A) and (B) indicated the concentration of 8-oxo-Gsn and 8-oxo-dGsn in urine increased with the passage of time by UHPLC-MS/MS, respectively. Creatinine (Cre) was used to normalize the oxidized guanosine level. All results are expressed as the mean±SEM. Statistical difference determined by the t-test. **p<0.01, 521 ****p<0.0001.

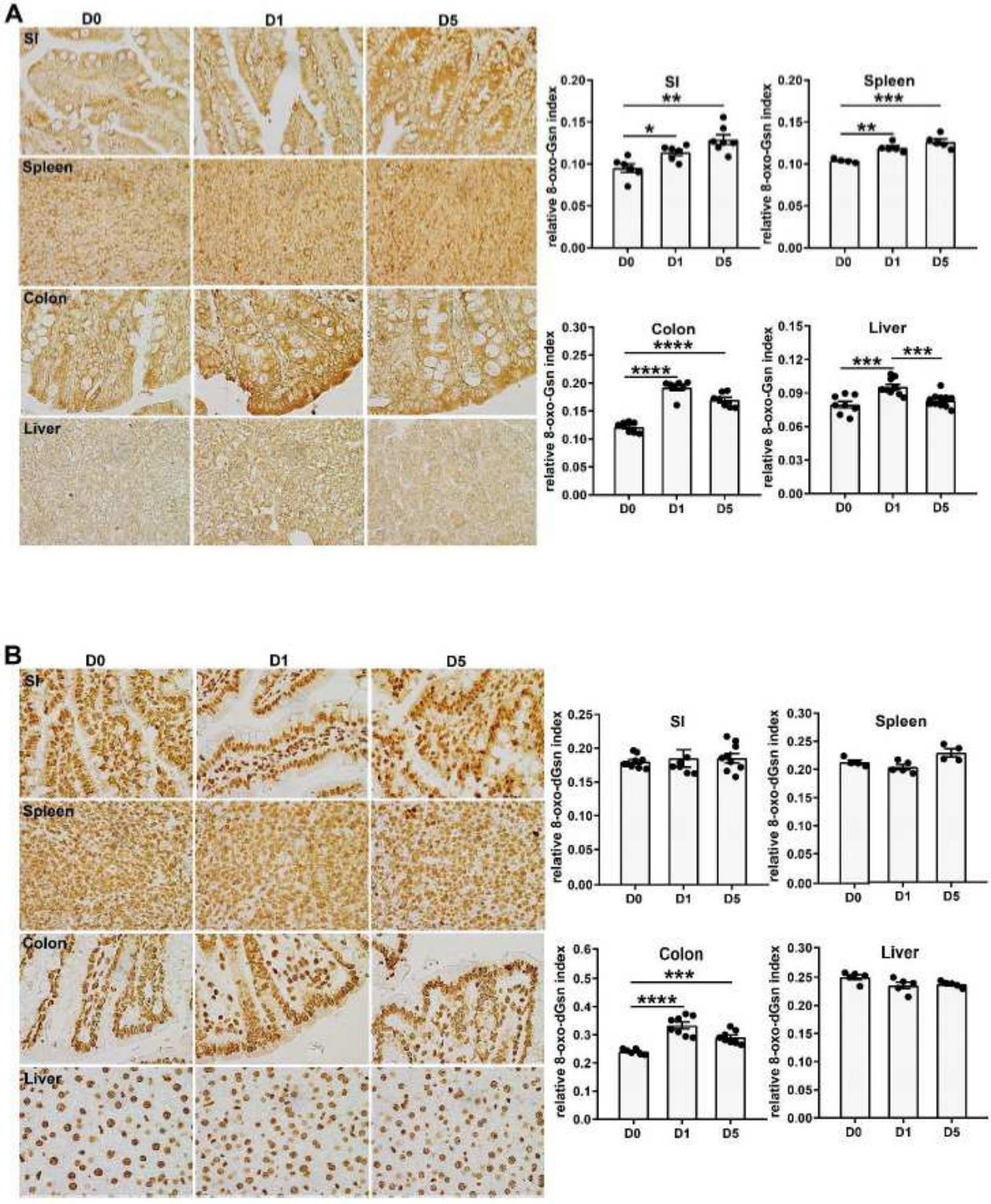

Figure 2

IHC determination for 8-oxo-dGsn in nuclear DNA and 8-oxo-Gsn in cellular RNA from tissues of rats. IHC stain for 8-oxo-Gsn in cellular RNA (A) and 8-oxo-dGsn in nuclear DNA (B) in small intestine (SI), spleen, colon and liver of SD rats at D0, D1, D5, respectively. All results are expressed as the mean±SEM. Significance determined using the t-test. *p<0.05, **p<0.01, ***p<0.001, ****p<0.0001.

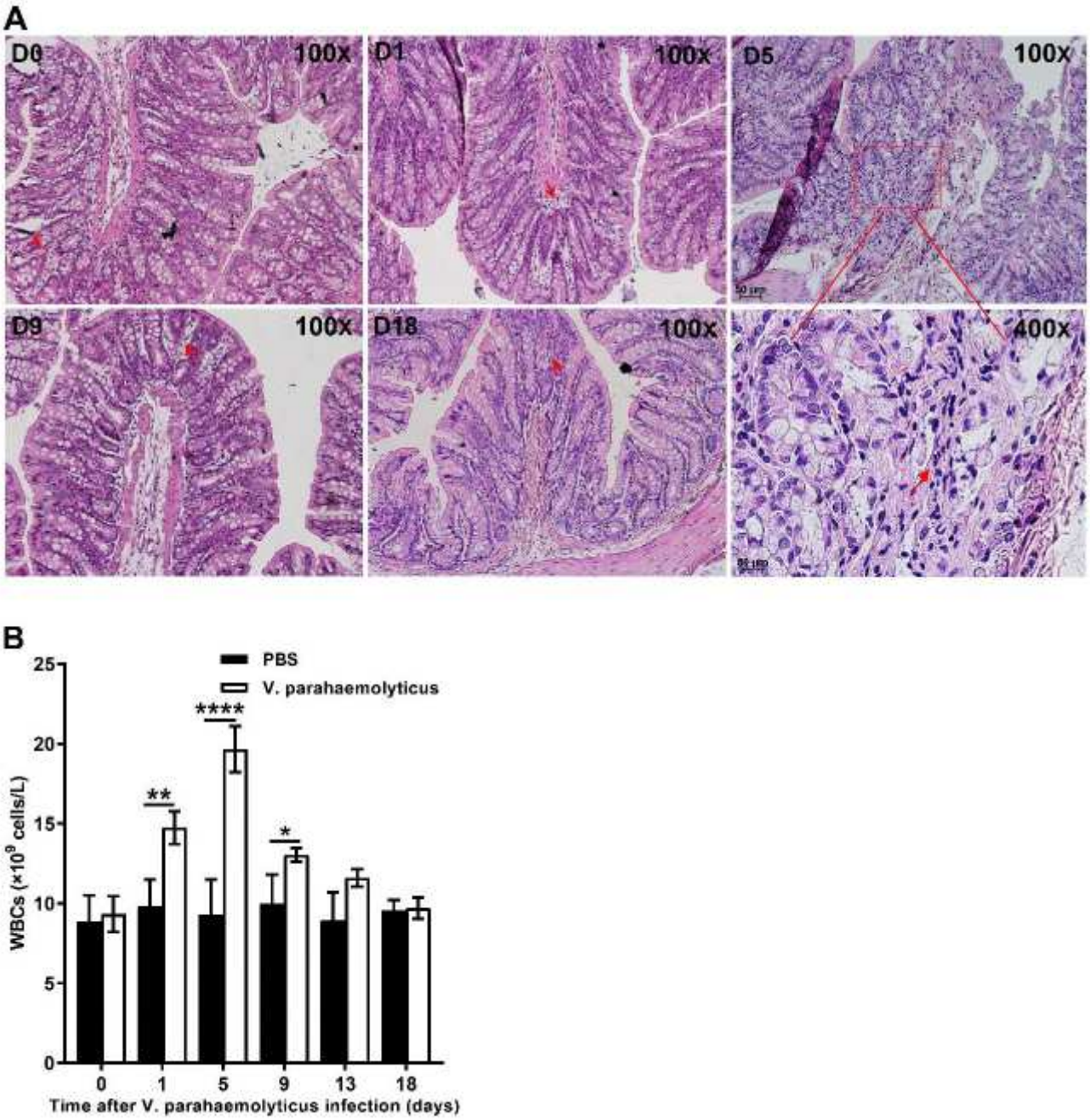

Figure 3

Inflammation heightened after infection with V. parahaemolyticus. (A) H&E stain of the colon of SD rats challenged with V. parahaemolyticus at D0, D1, D5, D9 531 and D18. The red arrows indicate the infiltration of lymphocytes in colon. Images were taken at ×100 magnification, except for the ×400 magnification zoomed-in local view at D5. (B) WBCs of SD rats with and without V. parahaemolyticus infection at D0, D1, D5, D9, D13 and D18. All results are expressed as the mean±SEM. Significance determined using the t-test. *p<0.05, **p<0.01, ****p<0.0001.

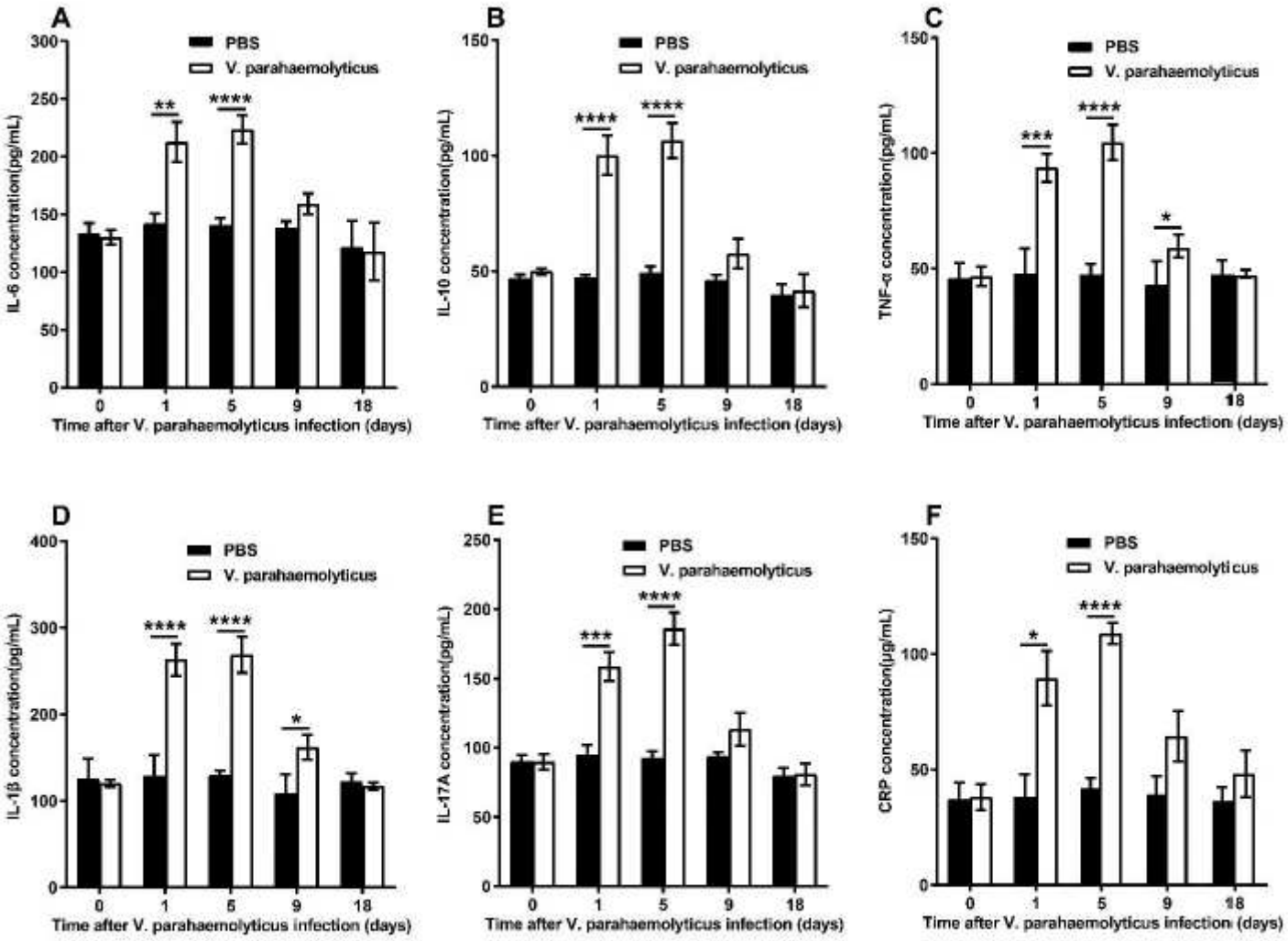

Figure 4

The concentration of inflammatory cytokines was increased after infection with V. parahaemolyticus. Luminex and ELISA were used to detect the concentration of IL-6, IL-10, TNF-α, IL-1β and IL-17A (A to E) and CRP (F), respectively. All results are expressed as the mean±SEM. Significance determined using the t-test. *p<0.05, 541 **p<0.01, ***p<0.001, ****p<0.0001.

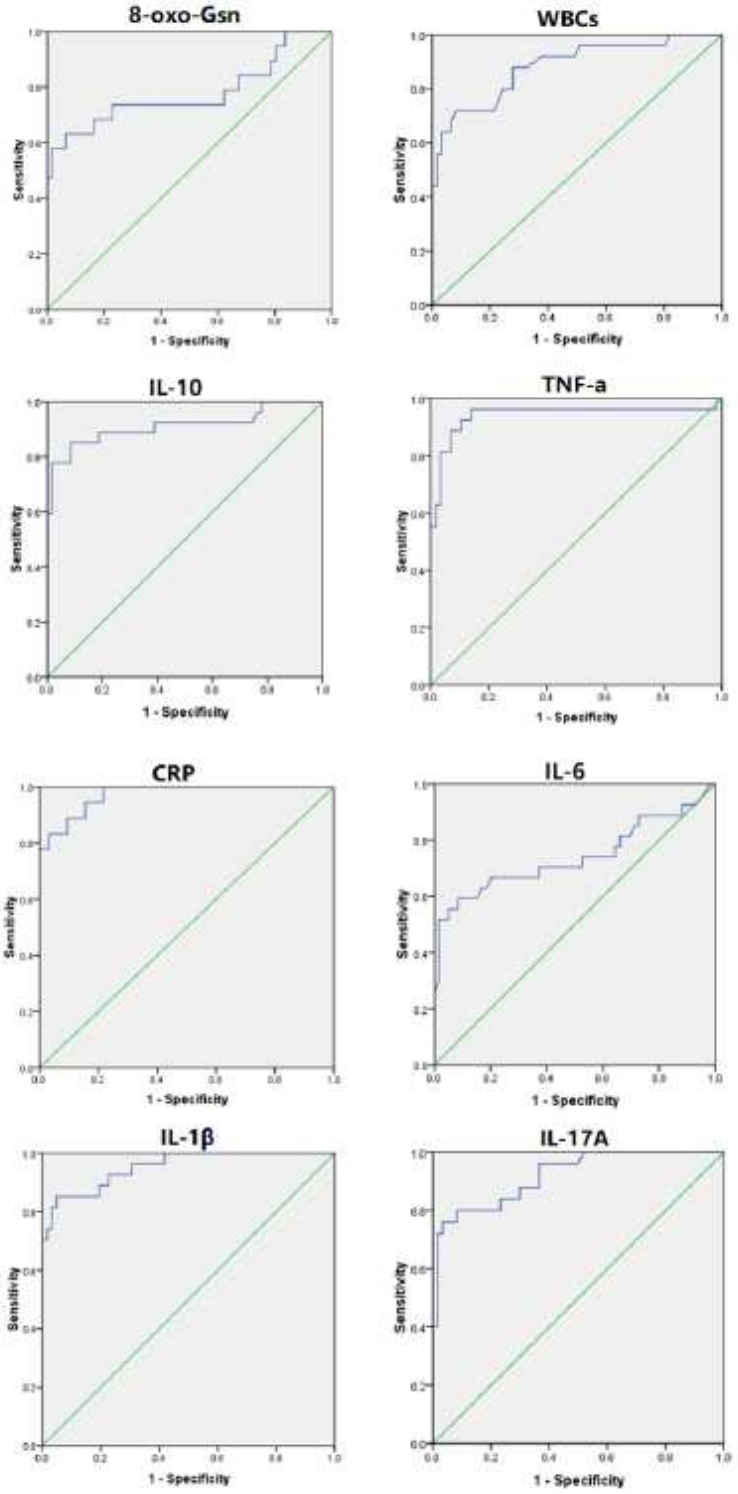

Figure 5

The area under receiver operator characteristic (ROC) curve of 8-oxo-Gsn, WBCs and inflammatory cytokines including CRP, IL-6, IL-10, TNF-α, IL-1β and IL-17A for assessing the infection status.

Supplementary Files

This is a list of supplementary files associated with this preprint. Click to download.

- FigureS3.jpg
- FigureS1.jpg
- FigureS2.jpg